RSC Advances

ROYAL SOCIETY OF CHEMISTRY

www.rsc.org/advances

Electrochemical Synthesis of Poly(3,4-ethylenedioxythiophene) in Aqueous Dispersion of High Porosity Reduced Graphene Oxide

Tom Lindfors [a,b*], *Zhanna Boeva* [a,c] *and Rose-Marie Latonen* [a]

[a] Åbo Akademi University, Process Chemistry Centre, Department of Chemical Engineering, Laboratory of Analytical Chemistry, Biskopsgatan 8, FIN-20500 Turku, Finland

[b] Academy of Finland, Helsinki

[c] M.V. Lomonosov Moscow State University, Chemistry Department, Polymer Division, Leninskie gory 1, build. 3, Moscow, Russian Federation

Abstract

We report here the one-step electrochemical synthesis of poly(3,4-ethylenedioxythiophene) (PEDOT) in an aqueous dispersion of reduced graphene oxide (rGO). The electrochemical polymerization is carried out at 1.05 V in aqueous media in the presence of 10^{-2} M 3,4-ethylenedioxythiophene and 1 g/l rGO. Unlike composites of PEDOT and graphene oxide or poly(styrene sulfonate) which have rather smooth and non-porous surface morphologies, the scanning electron microscopy images reveal that the PEDOT composite films obtained in this work have uniformly porous and open surface morphology. X-ray photoelectron spectroscopy (XPS) showed that rGO had initially a low concentration of oxygen-containing surface groups (C:O ratio=6.5), but both FTIR spectroscopy and XPS showed that the electropolymerization resulted in the formation of OH groups in the composite film. Characterization with cyclic voltammetry and electrochemical impedance spectroscopy demonstrates that the composite films behave almost like ideal capacitors having an areal capacitance of 12.2 mF cm^{-2}. The composite films had a very good potential cycling stability in 0.1 M KCl with only 12.4%

* Corresponding author. Tel. +358 2 2154419. E-mail: Tom.Lindfors@abo.fi (Tom Lindfors)

degradation of the capacitance in a three-electrode cell after 3000 cycles between -0.5 and 0.5 V. The degradation was higher (32.8%) in the broader potential range of -0.8 and 0.7 V.

1. Introduction

Graphene has great potential in several applications ranging from *e.g.* electronics, supercapacitors, flexible displays, touch screens, solar cells, chemical sensors, and biodiagnostics due to its one-atom thick 2-D structure and transparency, high specific surface area, good mechanical and electrical properties, and the possibility of functionalizing the graphene surface.[1-3] The exfoliation of graphite usually result in the formation of the water soluble and electrically non-conducting graphene oxide (GO) with oxygen-containing groups (hydroxyl, epoxy, carbonyl and carboxyl)[4] on the GO sheets which can be chemically reduced[5] with hydrazine[6], sodium borohydride,[7] strongly alkaline NaOH,[8] L-ascorbic acid,[9] sodium carbonate[10] or electrochemically at sufficiently negative potentials.[11-13] The reduction removes most of the surface groups of GO and converts it to the electrically conducting reduced graphene oxide (rGO) which is water insoluble (like graphene) complicating further processing of the rGO.

Composite materials of electrically conducting polymers (ECP) and graphene or rGO have a synergetic effect which improves, for example, the capacitance of the composite materials compared to the ECPs and graphene or rGO alone.[13] In the ECP-graphene and ECP-rGO composites, the graphene and rGO which are electrical double layer capacitors add mechanical strength to the ECP matrix and increase its electrical conductivity while the ECPs are redox capacitors (pseudocapacitors) improving the relatively low capacitance of graphene and rGO. This synergetic effect was reflected in the high capacitance of 1126 F g^{-1} obtained for the PANI-rGO composite,[14] in comparison to the much lower capacitance of the graphene

ultracapacitors, 135 F g^{-1},[15] and polyaniline (PANI) with a nanowire structure, 724 F g^{-1}.[16] It was also recently shown that the electrochemical reduction of PANI-GO to PANI-rGO improved the electroactivity with 30% and increased the areal capacitance with 15% from 67 mF cm^{-2} to 77 mF cm^{-2}.[13] Moreover, the PANI-GO composite film had an outstanding potential cycling stability in 0.1 M KCl for 10000 cycles between -0.5 to 0.5 V with no degradation of the anodic charge showing the beneficial effect of incorporating GO in the ECP matrix.

Among the ECPs, the poly(3,4-ethylenedioxythiophene) (PEDOT) has a very good environmental stability. It is difficult to reduce PEDOT to its electrically non-conducting form and it retains its electrical conductivity in a relatively wide potential window (*ca.* 1.0 V). Especially in supercapacitors, it is desirable to maximize the potential window because the energy (E) storage capacity in capacitors is proportional to the second power of the potential window ($E=0.5\times C\times U^2$; C and U are the capacitance and potential window, respectively). Therefore, most capacitors are operated in organic solvents to maximize the potential window and thus, the energy storage capacity. However, it is desirable to replace the organic solvents with more environmentally friendly alternatives. Moreover, compared to PANI, the specific capacitance of PEDOT is much lower varying between 30 to 170 F g^{-1} [17-21] but it maintains its electroactivity at neutral pH allowing the use of environmentally friendly and non-hazardous aqueous solvents. Very recently, it was reported that PEDOT synthesized in an ionic liquid (1-ethyl-3-methyl-imidazolium bis(trifluoromethylsulfonylimide, EMI-BTI)) with 0.36 C cm^{-2} had a relatively high areal capacitance of 10.5±1 mF cm^{-2} in a two-electrode cell and showed high stability over hundreds of thousands of potential cycles in EMI-BTI.[22] This is considerably higher than 26-52 μF cm^{-2} which was reported for graphene nanosheets in the three-electrode cell.[23] By combining PEDOT and CNTs, the areal capacitance was improved

to ca. 80 mF cm^{-2} for the composite film of PEDOT-CNT (prepared from an acetonitrile-aqueous mixture with 0.5 C cm^{-2}) demonstrating the synergistic effect of these two materials.[24]

Different variations of chemical oxidative polymerization have been usually used to synthesize PEDOT-GO and PEDOT-rGO resulting often in intractable and non-dispersible composite materials which hampers the further processing of these composites.[25-27] Electrochemical synthesis of PEDOT-GO was carried out only in a few cases. Recently, PEDOT was electrochemically polymerized from an aqueous solution with GO as the only charge compensating counter ion.[28, 29] During the electropolymerization, the incorporation of GO in the positively charged PEDOT matrix is possible mainly due to the polar epoxy and hydroxyl groups making the GO surface negatively charged. The electropolymerization of PEDOT-rGO is even less studied than for PEDOT-GO. PEDOT has been either electropolymerized on the surface of rGO [30] or GO has been electrochemically reduced to rGO on top of the electrochemically prepared PEDOT layer.[31] Electropolymerization of PEDOT-rGO composites have been reported from a colloidal ethanol dispersion of rGO.[32] However, the atomic composition of rGO was 58.85% carbon and 41.15% oxygen (C:O=1.4), thus having a C:O ratio characteristic for GO (2.1-4.1) .[5]

In this work, we report the electropolymerization of PEDOT in an aqueous dispersion of high porosity rGO having the C:O ratio 6.5. Unlike PEDOT-GO and PEDOT-PSS (poly(styrene sulfonate)), we show that the PEDOT composite films obtained in this work have porous and open surface morphology. X-ray photoelectron (XPS) and FTIR spectroscopy showed that the electropolymerization selectively enhanced the formation of OH groups in the composite film due to re-oxidation of rGO. The PEDOT composite films had good potential cycling stability

in a three-electrode cell for 3000 cycles. Moreover, the redox capacitances calculated from the cyclic voltammograms (CV) of the composite films indicate that their behavior closely resembles ideal capacitors with no scan rate dependence.

2. Results and discussion

2.1. Characterization of the PEDOT composite films

The CVs of the PEDOT composite films show that they closely resemble ideal capacitors at the scan rates of 20-200 mV s^{-1} (Figure 1). For these scan rates, the areal redox capacitances

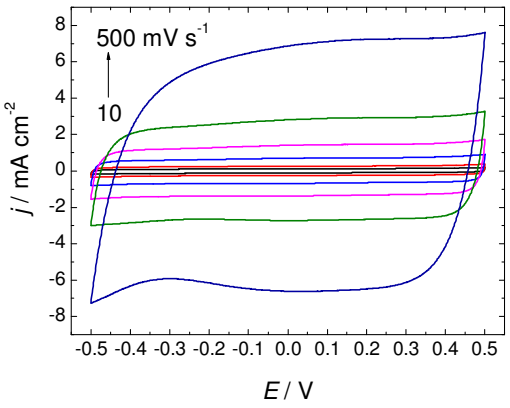

Figure 1. Cyclic voltammograms of the PEDOT composite film in 0.1 M KCl measured with the scan rates of 10, 20, 50, 100, 200 and 500 mV s^{-1}. The potentials are given vs. Ag/AgCl/4 M KCl.

were 12.8 (20), 13.4 (50), 13.4 (100) and 13.1 mF cm^{-2} (200 mV s^{-1}) indicating that the capacitance is almost independent of the scan rate. At 10 and 500 mV s^{-1}, the areal capacitances were slightly lower, 11.6 and 12.0 mF cm^{-2}, respectively. The areal capacitances were calculated from the anodic charge (Q_+) of the CVs divided by the electrode area. We

have used areal redox capacitances instead of specific capacitances (F g^{-1}) because the mass of thin composite films cannot be measured accurately. The CVs in Figure 1 reveal that the composite films are converted to their electrically conducting form already at *ca.* -0.5 V and the charging/discharging of the films is quick and reversible. At the scan rate of 200 mV s^{-1}, the films can be charged and discharged within 10 s within the potential interval of -0.5 – 0.5 V. For the highest scan rate of 500 mV s^{-1}, the broad oxidation and reduction peaks at ca. 0.2 V and 0.05 V, respectively, become more pronounced in the CV of the PEDOT composite film due to the diffusion limitation of the charge compensating counterions participating in the oxidation and reduction process of PEDOT.

The reason for the capacitor-like behavior is most likely the uniformly porous surface morphology of the PEDOT composite film induced by the wrinkled structure of the high porosity rGO (Figures 2a-c). In contrast to the relatively smooth surface of the composite films of PEDOT-GO (Figure 2d) and PEDOT-PSS (Figure 2e), the surface of the PEDOT composite film electrochemically polymerized in the presence of rGO has an open morphology with the grain size of *ca.* 200-800 µm (Figures 2b and 2c). The open structure makes it easier for charge compensating counter ions to diffuse to the film surface and into the bulk of the composite film which improves the charging/discharging properties of the composite film. The capacitor-like behavior of the PEDOT composite film was further confirmed by the electrochemical impedance spectroscopic (EIS) measurement at 0.25 V. In Figure 3a, the almost vertical shape of the impedance spectra obtained at low frequencies (10-100 mHz) indicate that the composite films have nearly a pure capacitive behavior. The line fitting[28] in Figure 3b show that the PEDOT composite film measured at 0.25 V had the areal redox capacitance of 12.2 mF cm^{-2} (r^2=0.9999) which is in rather good accordance with the areal redox capacitance of PEDOT-GO films electropolymerized at 0.94 V (14.3 mF cm^{-2})

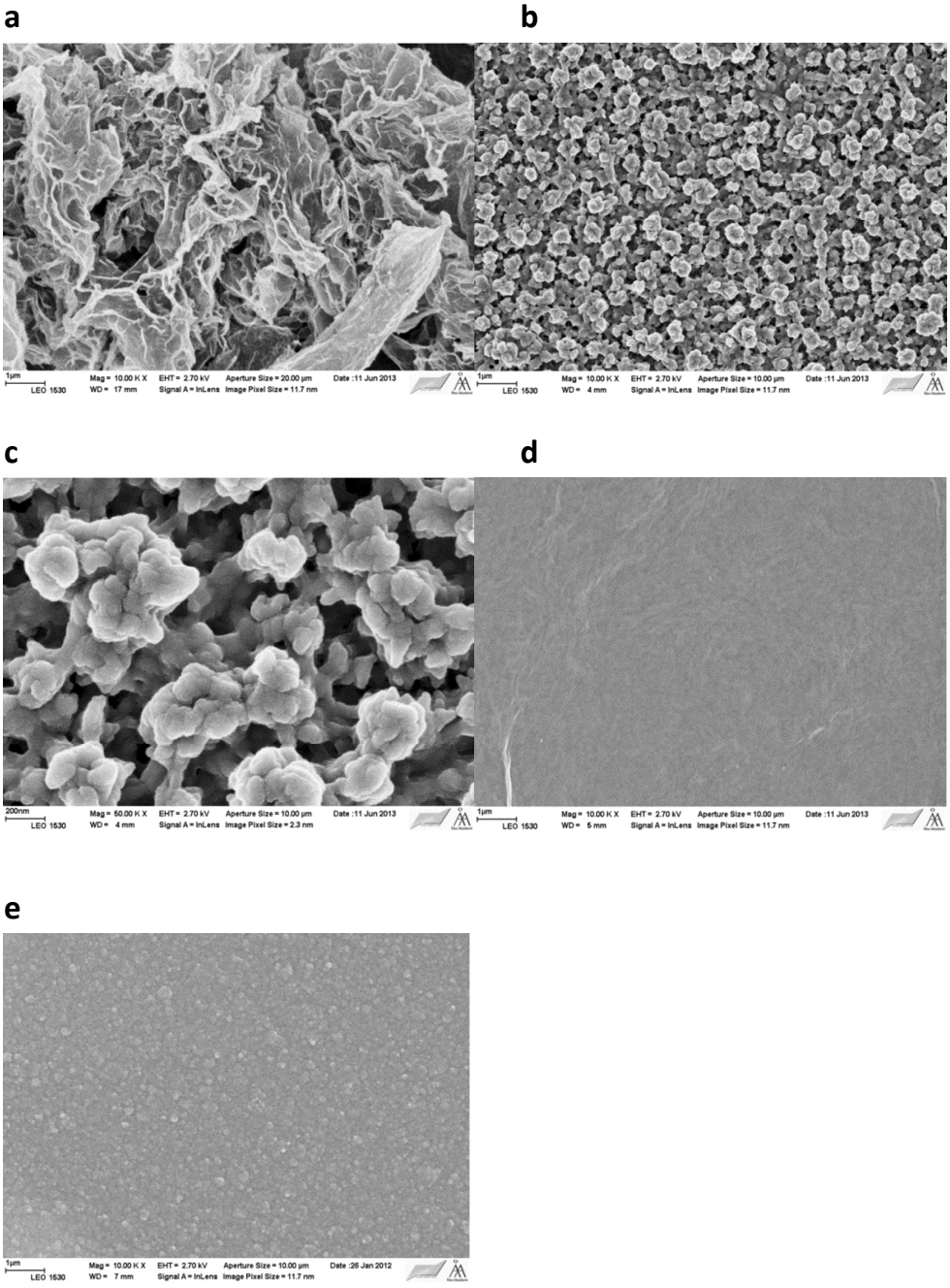

Figure 2. SEM images of the **(a)** rGO powder, **(b, c)** PEDOT composite, **(d)** PEDOT-GO and **(e)** PEDOT-PSS films. Magnification: 10000 x except of (c) which is measured with 50000 x.

and 0.97 V (14.7 mF cm^{-2}), but considerably higher than for PEDOT-GO prepared at 1.05 V (5.3 mF cm^{-2}).[29]

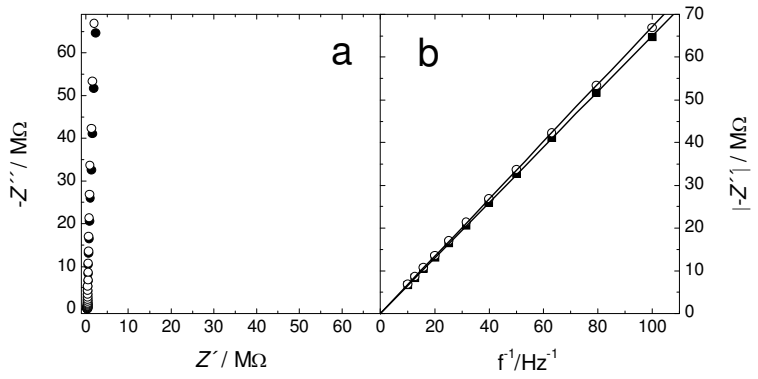

Figure 3. (a) The impedance spectra of the PEDOT composite film in 0.1 M KCl before (●) and after (○) the potential cycling stability test. **(b)** |-Z´´| vs f^{-1} plotted in the frequency range of 10-100 mHz. The electrodes were pretreated for 60 s at 0.25 V (vs. Ag/AgCl/4 M KCl) before starting the EIS measurement; f=100 kHz – 10 mHz, ΔE_{ac}=5 mV.

In Figure 4a, the Raman spectrum of rGO is shown with the D and G bands at 1346 and 1588 cm^{-1}, respectively. The Raman spectra of the PEDOT-PSS and the PEDOT composite films are almost identical verifying that the electropolymerization of (3,4-ethylenedioxythiophene) (EDOT) in the presence of rGO results in the formation of PEDOT (Figures 4b and 4c). The main bands in the Raman spectra of PEDOT-PSS and the PEDOT composite film are assigned to the asymmetric (1504/1499 cm^{-1}) and symmetric (1430/1435) C=C stretching, C_β-C_β stretching (1363/1366), C_α-$C_{\alpha'}$ inter-ring stretch (1259/1268), C-O-C deformation (1101/1098) and oxyethylene ring deformation (985/989).[33, 34] ECPs typically show strong Raman bands in the wavenumber region of the D and G bands which makes it difficult to verify the presence of these bands in the composite material.[28] However, the small shoulders

at *ca.* 1315 and 1605 cm^{-1} in the Raman spectrum of the PEDOT composite film indicate that the high porosity rGO was incorporated into the PEDOT matrix during the electropolymerization (Fig. 4c). Similar shoulders in the Raman spectra was previously observed for PEDOT-GO which was interpreted as originating from incorporation of GO in the PEDOT matrix.[28]

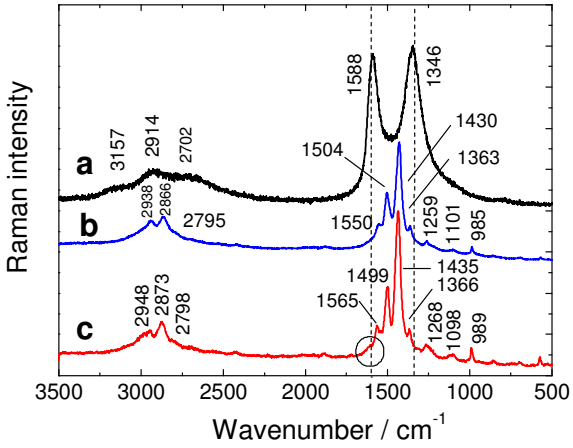

Figure 4. The Raman spectra of **(a)** the rGO powder, **(b)** the PEDOT-PSS and **(c)** the PEDOT composite films. Laser excitation wavelength: 514 nm.

To gain a deeper understanding of the PEDOT composite material, we measured the XPS spectra of rGO and the composite film (Figure 5). Except of the C-C/C=C band at 284.8 eV,[6, 9, 35] the C 1s spectra of rGO revealed that it contained low amounts of hydroxyl and epoxy (286.5 eV),[9, 35] carbonyl (287.6 eV)[6, 9, 35] and carboxyl (288.9 eV)[6, 35] groups (Figure 5a). The XPS fitting gave the following atomic composition of rGO: 83.4% carbon, 12.8% oxygen, 3.6% nitrogen and 0.2% sulfur which gives a C:O ratio of 6.5. It has been shown that reduction of GO with hydrazine results in the formation of C-N groups on the rGO surface.[7]

According to ref. 7, the reduction of GO with 50 mM hydrazine resulted in the C:O ratio of 6.2 and the nitrogen content of 2.4%. It is therefore likely that the nitrogen in the high porosity rGO originates from reduction with hydrazine which can be seen as a C-N band at 285.7 eV in the C 1s XPS spectrum of rGO [28, 35] (Figure 5a). In addition to the C 1s spectrum, the O 1s spectrum confirm the presence of carbonyl and carboxyl (531.3 eV), and hydroxyl and epoxy (532.1 eV) groups on the rGO surface, but also that some amounts of carbonyl and epoxy oxygens are bound to ester groups (533.5 eV) [36] (Figure 5b).

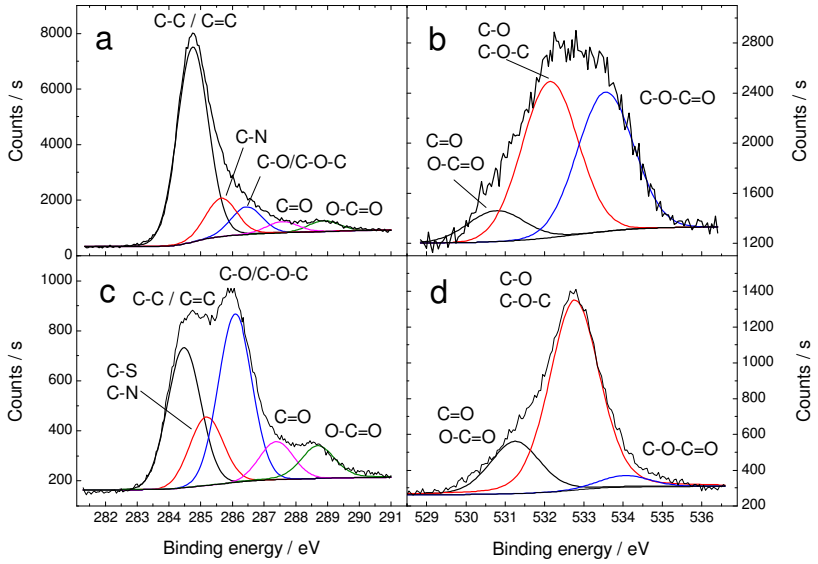

Figure 5. XPS spectra of **(a, b)** the rGO powder and **(c, d)** the PEDOT composite film. (a) and (c): C 1s spectra (χ^2=2.1 and 2.5, respectively); (b) and (d): O 1s spectra (χ^2=1.6 and 2.1, respectively).

The XPS spectrum of the PEDOT composite shows a relatively intense hydroxyl/epoxy/ether band at 286.1 eV except of the C-C/C=C (284.5 eV), C-N/C-S (285.2 eV), carbonyl (287.4 eV) and carboxyl (288.7 eV) bands (Figure 5c). Also, the intensity of the hydroxyl/epoxy/ether band at 532.8 eV in the O 1s spectrum of the composite increased in

relation to the carbonyl and carboxyl band (531.3 eV) and the band assigned to the carbonyl and ether oxygens in ester groups (534.1 eV) (Figure 5d). It is expected that the C-O-C band of the PEDOT composite material has a higher intensity than rGO due to the ether groups in the PEDOT structure. However, compared to the intensity of the C-O-C band in the XPS spectrum of PEDOT-PSS (Figure S1b) which is much lower than for the PEDOT composite film prepared from the rGO dispersion, the increase of the intensity of the C 1s band at 286.1 eV of the composite film cannot only be explained by the increase of the ether bonds originating from PEDOT. It can therefore be speculated that the electropolymerization which is carried out under nitrogen at the relatively high potential of 1.05 V and slightly alkaline conditions (pH=8.9) will result in formation of peroxide and hydroxyl radicals due to partial electrolysis of water. Consequently, this can favor re-oxidation of the rGO and the formation of OH groups on its surface. For comparison in PEDOT-GO (Figure S1a), the high content of hydroxyl and epoxy groups are seen as a strong band in the XPS spectrum at 286.9 eV.[28] The XPS fitting unveil that PEDOT-GO and the PEDOT composite in this work have almost similar carbon (68.1/65.8%) and oxygen (28.8/25.8%) contents which corresponds to the C:O ratios of 2.4 (PEDOT-GO) and 2.6 (PEDOT composite) further supporting the assumption of re-oxidation of the rGO surface during the electropolymerization. The electrosynthesis of the PEDOT composite film (0.5 C cm^{-2}) takes *ca.* 50 min (on glassy carbon (GC) electrodes with d=1.6 mm) which provides enough time for the surface reactions to take place. If the increased oxygen content of the PEDOT composite film would originate from overoxidation of the PEDOT matrix, this would be seen as an increase in the C=O band intensity in both the C 1s and O 1s spectrum.[37] Hence, since this is not the case, the re-oxidation of the rGO seems as the most plausible explanation to the increased oxygen content in the PEDOT composite film. Nevertheless, the combination of EDOT and the high porosity rGO as starting materials,

and the re-oxidation of rGO creates a PEDOT composite film with completely open surface morphology, ideal capacitor-like behavior and fast charging/discharging properties.

The FTIR spectra of rGO in Figure 6 (spectrum a) is almost featureless except of the bands related to the absorption of crystal water at 532 cm^{-1} and 631 cm^{-1}, and the vibrational bands at 777, 1065 and 1163 cm^{-1} bands originating from the carbon-hydroxo complexes of rGO and coordinated water.[38] This is in good accordance with the XPS spectrum of rGO in Figures 5a and 5b confirming the low amount of hydroxyl, epoxy, carbonyl and carboxylic groups in rGO. In Figure 6 (spectrum b), the FTIR spectrum of the PEDOT composite shows

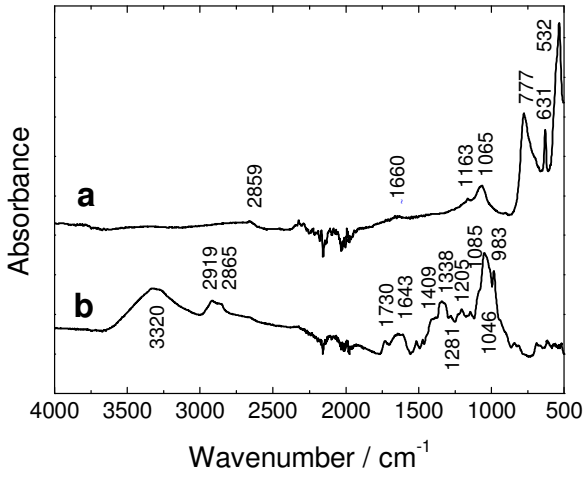

Figure 6. The FTIR spectra of **(a)** the rGO powder and **(b)** the PEDOT composite film.

bands originating from OH stretching and absorbed water (3320 cm^{-1}), -C=O stretching of carboxylic and carbonyl groups (1730 cm^{-1}),[39, 40] C-OH deformation (1409 cm^{-1}), C-O-C (1205 cm^{-1}) and C-O groups (1046 cm^{-1}).[41, 42] The rather broad band at 1643 cm^{-1} is most

likely related to skeletal vibrations of graphitic (sp^2) domains or bending vibrations of water molecules.[38, 41] The main IR bands of PEDOT are usually located below 1550 cm^{-1} and are so called doping induced bands (983, 1085, 1281, 1338 cm^{-1}).[43-45] A more thorough discussion of the FTIR bands of PEDOT-GO is given in ref. 25. It can be concluded from the FTIR spectrum b in Figure 6 that the electropolymerization process results in formation of PEDOT and the bands at 1046, 1409 and 3320 cm^{-1} indicate that OH groups are formed on the re-oxidized rGO surface. Moreover, the band at 1730 cm^{-1} assigned to carboxyl and carbonyl stretching may indicate a certain degree of overoxidation of the PEDOT matrix.

2.2. Potential cycling stability

To increase the potential window of the PEDOT composite film in 0.1 M KCl, the film was first cycled from 0.5 V to different cathodic end potentials (-0.5 to -1.0 V) to study its oxidation and reduction behavior (Figure 7a). The CVs in Figure 7a demonstrate that the composite film converts to the electrically conducting form at *ca.* -0.8 V (the current density

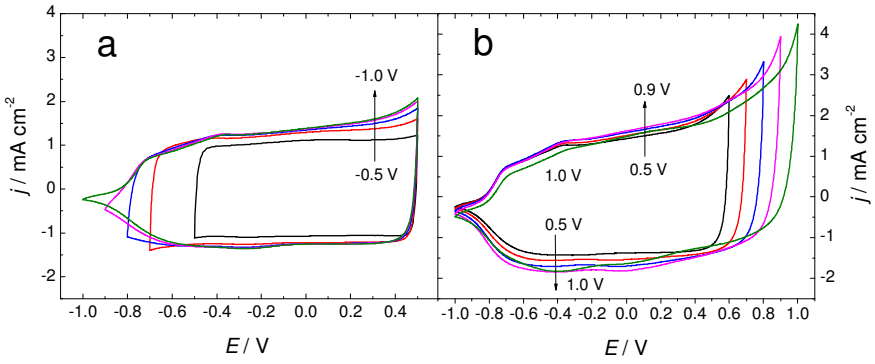

Figure 7. Cyclic voltammograms of the PEDOT composite films measured in 0.1 M KCl, v=100 mV s^{-1}. Anodic and cathodic potential limits: **(a)** 0.5 V and -1.0/-0.9/-0.8/-0.7/-0.5 V (vs. Ag/AgCl/4 M KCl), respectively. **(b)** 0.6/0.7/0.8/0.9/1.0 V and -0.5 V, respectively.

becomes positive). This potential is 0.3 V more negative than the cathodic end potential of -0.5 V which is usually used in potential cycling of PEDOT in aqueous media. To extend the cathodic/anodic end potentials to more negative/positive potentials will be beneficial for improving the energy storage capacity of the PEDOT composite film. Figure 7b shows the influence of the anodic end potential on the CV of the composite film in 0.1 M KCl. The potential cycling was started at -1.0 V and continued to the anodic end potential of 0.6 – 1.0 V. The CVs reveal a rather sharp increase in the anodic current as the potential exceeds 0.5 V. To avoid overoxidation of the PEDOT composite film, the anodic potential limit of 0.7 V was therefore chosen for the potential cycling stability test which was conducted in the potential interval of -0.8 – 0.7 V. The results of this test were compared with the cycling stability in the more narrow potential interval between -0.5 – 0.5 V.

The results of the potential cycling stability tests are presented in Figures 8a and 8b. As shown in Figure 8a, the potential cycling stability of the PEDOT composite film is very good for at least 3000 cycles between -0.5 – 0.5 V in 0.1 M KCl with only 12.4% decrease of the areal capacitance from 12.1 mF cm^{-2} to 10.6 mF cm^{-2} (Figure 9). The stability against degradation was even better between 200-3000th cycles (capacitance decrease: 7.8%), if the initial conditioning and structural re-orientation effects of the composite film are neglected during the first 200 potential cycles. After the stability test, the film relaxation was allowed to take place at the open circuit potential before recording the EIS spectra at 0.25 V. The obtained areal capacitance of 11.8 mF cm^{-2} (3.3% decrease of its initial value; r^2=1) further confirmed the good stability against degradation of the PEDOT composite film (Figure 3). It must be stressed that the CV of the PEDOT composite film in Figure 8a shows almost a

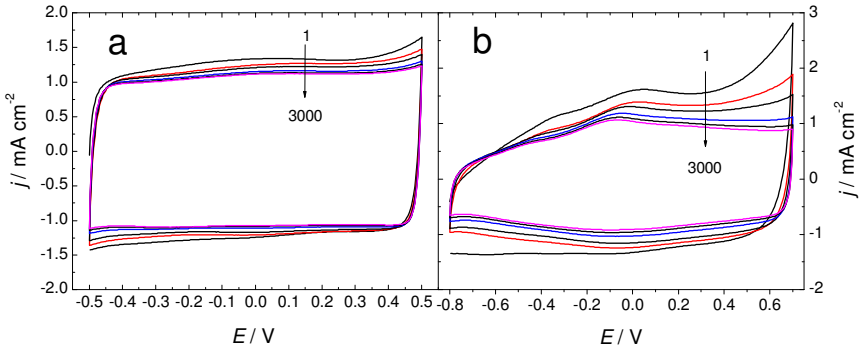

Figure 8. Cyclic voltammograms of the PEDOT composite film measured during the potential cycling stability test in 0.1 M KCl under nitrogen, v=100 mV s^{-1}. Potential interval: **(a)** -0.5 V to 0.5 V, **(b)** -0.8 V to 0.7 V. The 1, 50 (red line), 200, 1000 (blue), 2000 and 3000th (magenta) cycles are shown in the figure.

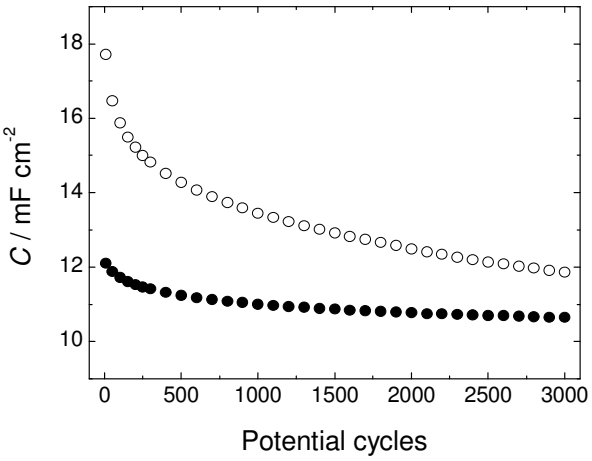

Figure 9. The areal capacitance vs. the number of potential cycles for the PEDOT composite film recorded during the potential cycling stability test shown in Figure 8. Potential interval: (●) -0.5 V to 0.5 V, (○) -0.8 V to 0.7 V.

rectangular shape characteristic of ideal capacitors. Most likely the re-oxidized rGO surface can act as charge compensating counter ions during the oxidation and reduction process of the composite film which decreases the diffusion pathway of the counter ions to the PEDOT matrix, thus ensuring a quick charging/discharging of the material. This effect is probably enhanced by the fully open film structure facilitating the diffusion of the chloride ions from the electrolyte solution into the entire bulk of the polymer matrix.

The areal capacitance of the PEDOT composite film was improved when the potential cycling was done between -0.8 – 0.7 V (Figures 8b and 9). In the beginning of the potential cycling stability test, the areal capacitance was 17.7 mF cm^{-2} which is *ca.* 46% higher than the capacitance value obtained in the potential interval of -0.5 – 0.5 V (Figure 9). However, the areal capacitance decreases quickly especially during the first 200 potential cycles which is reflected as a decrease in the oxidation and reduction currents in the CV of the composite film (Figure 8b). By neglecting the initial capacitance decrease for the first 200 potential cycles, the areal capacitance decreases with 21.7% during the rest of the stability test (200-3000th cycles). It can be speculated that the continuous potential cycling of the PEDOT composite film to 0.7 V partially overoxidizes the polymer which results in the decrease of the oxidation and reduction currents observed in the CV in Figure 8b, and consequently, in a lower areal capacitance. However, the composite film showed still a reasonably good areal capacitance of 11.9 mF cm^{-2} after 3000 potential cycles between -0.8 – 0.7 V (Figure 9).

3. Experimental

3.1 Electropolymerization

The electropolymerization at 1.05 V (vs. Ag/AgCl/4 M KCl) was carried out to the charge density of 0.5 C cm^{-2} in an aqueous dispersion of rGO (1 g L^{-1}) and 0.01 M EDOT at pH 8.9. Deionized water was first added to the high porosity rGO powder before EDOT was added to the dispersion which was purged with nitrogen for 15 min before starting the electropolymerization. The high porosity rGO was purchased from Graphene Supermarket (specific surface area: ~400 m^2 g; average flake thickness: 1 monolayer; average lateral particle size: ~3-10 µm). The PEDOT composite films were formed in a three-electrode cell on GC (d=1.6 or 3.0 mm) electrodes incorporated in PEEK bodies while a GC rod functioned as the counter electrode. At lower electrode potentials than 1.05 V the film growth was very slow.

3.2 Cyclic voltammetry and electrochemical impedance spectroscopy

After the polymerization, the PEDOT composite films were characterized in oxygen-free 0.1 M KCl with cyclic voltammetry and electrochemical impedance spectroscopy. The CVs and impedance spectra were measured with an Autolab potentiostat equipped with the FRA module. The EIS spectra were recorded at 0.25 V (vs. Ag/AgCl/4 M KCl) in the frequency range of 100 kHz−10 mHz with ΔE_{ac}=5 mV. The composite films were conditioned at 0.25 V for 60 s prior to the EIS measurement.

3.3 Scanning electron microscopy (SEM) and X-ray photoelectron spectroscopy

The SEM images were recorded with a LEO 1530 Gemini FEG-SEM instrument and the XPS spectra were collected using a Phi Quantum 2000 (Physical Electronics) instrument with monochromatized Al Kα as the radiation source.

3.4 FTIR-ATR and Raman spectroscopy

The FTIR-ATR spectra were recorded using a Harrick's VideoMVP™ single reflection diamond ATR accessory (incidence angle: 45°) having a horizontal sampling area (diameter: 500 µm) and a built-in pressure applicator. All the analyzed films were tightly pressed against the diamond crystal during the spectral measurement. The VideoMVP™ ATR accessory was mounted in the Bruker IFS 66S spectrometer equipped with the DTGS detector. Totally 32 interferograms were co-added for each spectrum (resolution: 4 cm^{-1}).

All Raman measurements were carried out with the 514 nm laser (LaserPhysics, Ar ion laser) connected to a Leica DMLM and Renishaw Raman imaging microscope (equipped with the Wire™ v1.3 Raman software). The spectrometer was calibrated against a Si-standard (520.0 cm^{-1}) before measuring the Raman spectra of each composite film with 1% of the maximum laser power (20 mW) by accumulating 10 spectra.

3.5 Potential cycling stability

In a three-electrode cell, the potential cycling stability was measured in oxygen-free 0.1 M KCl (20 mL) by cycling the potential for 3000 cycles either between -0.5 – 0.5 V or -0.8 – 0.7 V (vs. Ag/AgCl/4 M KCl) with the scan rate of 100 mV s^{-1}. The solution was sealed and was blanketed with a low nitrogen gas flow during the entire stability test.

4. Conclusions

The electrosynthesis of PEDOT at 1.05 V in an aqueous dispersion of rGO results in the formation of C-O groups in the composite film having a fully open surface morphology. It is likely that re-oxidation of the rGO surface occurs during the electropolymerization at the relatively high polymerization potential and OH groups are formed on its surface. The re-oxidized rGO flakes can therefore act as charge compensating counter ions favoring the film formation. CV measurements showed that the electrochemical behavior of the composite film

closely resembles an ideal capacitor with almost no scan rate dependence (20-200 mV s^{-1}). This is probably due to the combination of the unique open film structure and the charge compensation process which efficiently shortens the diffusion pathways of the counter ions in the PEDOT matrix. In a three-electrode cell, the potential cycling stability tests demonstrated that the PEDOT composite film had very good stability for 3000 cycles in 0.1 M KCl with only 12.4% decrease in the areal capacitance from its initial value of 12.1 mF cm^{-2} when the potential was cycled between -0.5 V and 0.5 V. Due to its reversible redox properties and good electrochemical stability it is expected that the PEDOT composite films can be applied as ion-to-electron transducers in solid-state devices.

Acknowledgments

Dr. Anna Österholm at Georgia Institute of Technology (USA), Assoc. Prof. Róbert E. Gyurcsányi at the Budapest University of Technology and Economics (Hungary) and Lic. Fil. Jyrki Juhanoja (Finland, Top Analytica Ltd.) are gratefully acknowledged for fruitful discussions and advices. T.L. acknowledges the Academy of Finland for financial support (project number 130588).

Figure captions

Figure 1. Cyclic voltammograms of the PEDOT composite film in 0.1 M KCl measured with the scan rates of 10, 20, 50, 100, 200 and 500 mV s^{-1}. The potentials are given vs. Ag/AgCl/4 M KCl.

Figure 2. SEM images of the **(a)** rGO powder, **(b, c)** PEDOT composite, **(d)** PEDOT-GO and **(e)** PEDOT-PSS films. Magnification: 10000 x except of (c) which is measured with 50000 x.

Figure 3. (a) The impedance spectra of the PEDOT composite film in 0.1 M KCl before (●) and after (○) the potential cycling stability test. **(b)** |-Z´´| vs f^{-1} plotted in the frequency range of 10-100 mHz. The electrodes were pretreated for 60 s at 0.25 V (vs. Ag/AgCl/4 M KCl) before starting the EIS measurement; f=100 kHz – 10 mHz, ΔE_{ac}=5 mV.

Figure 4. The Raman spectra of **(a)** the rGO powder, **(b)** the PEDOT-PSS and **(c)** the PEDOT composite films. Laser excitation wavelength: 514 nm.

Figure 5. XPS spectra of **(a, b)** the rGO powder and **(c, d)** the PEDOT composite film. (a) and (c): C 1s spectra (χ^2=2.1 and 2.5, respectively); (b) and (d): O 1s spectra (χ^2=1.6 and 2.1, respectively).

Figure 6. The FTIR spectra of **(a)** the rGO powder and **(b)** the PEDOT composite film.

Figure 7. Cyclic voltammograms of the PEDOT composite films measured in 0.1 M KCl, v=100 mV s^{-1}. Anodic and cathodic potential limits: **(a)** 0.5 V and -1.0/-0.9/-0.8/-0.7/-0.5 V (vs. Ag/AgCl/4 M KCl), respectively. **(b)** 0.6/0.7/0.8/0.9/1.0 V and -0.5 V, respectively.

Figure 8. Cyclic voltammograms of the PEDOT composite film measured during the potential cycling stability test in 0.1 M KCl under nitrogen, v=100 mV s^{-1}. Potential interval: **(a)** -0.5 V to 0.5 V, **(b)** -0.8 V to 0.7 V. The 1, 50 (red line), 200, 1000 (blue), 2000 and 3000^{th} (magenta) cycles are shown in the figure.

Figure 9. The areal capacitance vs. the number of potential cycles for the PEDOT composite film recorded during the potential cycling stability test shown in Figure 8. Potential interval: (●) -0.5 V to 0.5 V, (○) -0.8 V to 0.7 V.

References

1 V. Singh, D. Joung, L. Zhai, S. Das, S. I. Khondaker and S. Seal, *Progr. Mater. Sci.*, 2011, **56**, 1178.

2 Y. W. Zhu, S. Murali, W. W. Cai, X. S. Li, J. W. Suk, J. R. Potts and R. S. Ruoff, *Adv. Mater.*, 2010, **22**, 3906.

3 T. Kuilla, S. Bhadra, D. H. Yao, N. H. Kim, S. Bose and J. H. Lee, *Progr. Polym. Sci.*, 2010, **35**, 1350.

4 D. R. Dreyer, S. Park, C. W. Bielawski and R. S. Ruoff, 2010, **39**, 228.

5 S. F. Pei and H. M. Cheng, *Carbon*, 2012, **50**, 3210.

6 S. Stankovich, R. D. Piner, X. Q. Chen, N. Q. Wu, S. T. Nguyen and R. S. Ruoff, *J. Mater. Chem.*, 2006, **16**, 155.

7 H. J. Shin, K. K. Kim, A. Benayad, S. M. Yoon, H. K. Park, I. S. Jung, M. H. Jin, H. K. Jeong, J. M. Kim, J. Y. Choi and Y. H. Lee, *Adv. Funct. Mater.*, 2009, **19**, 1987.

8 X. B. Fan, W. C. Peng, Y. Li, X. Y. Li, S. L. Wang, G. L. Zhang and F. B. Zhang, *Adv. Mater.*, 2008, **20**, 4490.

9 J. L. Zhang, H. J. Yang, G. X. Shen, P. Cheng, J. Y. Zhang and S. W. Guo, *Chem. Commun.*, 2010, **46**, 1112.

10 Y. H. Jin, S. Huang, M. Zhang, M. Q. Jia and D. Hu, *Appl. Surf. Sci.*, 2013, **268**, 541.

11 G. K. Ramesha and S. Sampath, *J. Phys. Chem. C*, 2009, **113**, 7985.

12 A. Viinikanoja, Z. J. Wang, J. Kauppila and C. Kvarnström, *PCCP*, 2012, **14**, 14003.

13 T. Lindfors and R.-M. Latonen, *Carbon*, 2014, **69**, 122.

14 H. L. Wang, Q. L. Hao, X. J. Yang, L. D. Lu and X. Wang, *Nanoscale*, 2010, **2**, 2164.

15 M. D. Stoller, S. J. Park, Y. W. Zhu, J. H. An and R. S. Ruoff, *Nano Lett.*, 2008, **8**, 3498.

16 V. Gupta and N. Miura, *Electrochem. Solid-State Lett.*, 2005, **8**, A630.

17 K. Lota, V. Khomenko and E. Frackowiak, *J. Phys. Chem. Solids*, 2004, **65**, 295.

18 J. Jang, J. Bae and E. Park, *Adv. Mater.*, 2006, **18**, 354.

19 Y. Li, B. C. Wang, H. M. Chen and W. Feng, *J. Power Sources*, 2010, **195**, 3025.

20 R. Liu, S. Il Cho and S. B. Lee, *Nanotechnology*, 2008, **19**.

21 W. K. Li, J. Chen, J. J. Zhao, J. R. Zhang and J. J. Zhu, *Mater. Lett.*, 2005, **59**, 800.

22 A. M. Österholm, D. E. Shen, A. L. Dyer and J. R. Reynolds, *ACS Appl. Mater. Inter.*, 2013, **5**, 13432.

23 X. Du, P. Guo, H. Song and X. Chen, *Electrochim. Acta*, 2010, **55**, 4812.

24 C. Peng, G. A. Snook, D. J. Fray, M. S. P. Shaffer and G. Z. Chen, *Chem. Commun.*, 2006, 4629.

25 S. Biswas and L. T. Drzal, *Chem. Mater.*, 2010, **22**, 5667.

26 J. T. Zhang and X. S. Zhao, *J. Phys. Chem. C*, 2012, **116**, 5420.

27 X. B. Yan, J. T. Chen, J. Yang, Q. J. Xue and P. Miele, *ACS Appl. Mater. Inter.*, 2010, **2**, 2521.

28 A. Österholm, T. Lindfors, J. Kauppila, P. Damlin and C. Kvarnström, *Electrochim. Acta*, 2012, **83**, 463.

29 T. Lindfors, A. Österholm, J. Kauppila and M. Pesonen, *Electrochim. Acta*, 2013, **110**, 428.

30 F. Jiang, Z. Yao, R. Yue, Y. Du, J. Xu, P. Yang and C. Wang, *Int. J. Hydrogen Energy*, 2012, **37**, 14085.

31 J. R. F. Foronda, S. M. R. Cabrera, D. L. Cumpas, P. G. A. Villar, J. L. Tan and B. J. V. Tongol, *Journal of Chemistry*, 2013.

32 A. P. Saxena, M. Deepa, A. G. Joshi, S. Bhandari and A. K. Srivastava, *ACS Appl. Mater. Interfaces*, 2011, **3**, 1115.

33 S. Garreau, G. Louarn, J. P. Buisson, G. Froyer and S. Lefrant, *Macromolecules*, 1999, **32**, 6807.

34 M. Lapkowski and A. Pron, *Synth. Met.*, 2000, **110**, 79.

35 H. Bai, Y. X. Xu, L. Zhao, C. Li and G. Q. Shi, *Chem. Commun.*, 2009, 1667.

36 G. P. Lopez, D. G. Castner and B. D. Ratner, *Surf. Interface Anal.*, 1991, **17**, 267.

37 P. Tehrani, A. Kanciurzewska, X. Crispin, N. D. Robinson, M. Fahlman and M. Berggren, *Solid State Ionics*, 2007, **177**, 3521.

38 G. Socrates, *Infrared and Raman characteristic group frequencies: tables and charts*, Wiley, Chichester; New York, 2001.

39 T. Szabó, O. Berkesi, P. Forgo, K. Josepovits, Y. Sanakis, D. Petridis and I. Dekany, *Chem. Mater.*, 2006, **18**, 2740.

40 T. Szabo, E. Tombacz, E. Illes and I. Dekany, *Carbon*, 2006, **44**, 537.

41 Y. Si and E. T. Samulski, *Nano Lett.*, 2008, **8**, 1679.

42 M. Acik, G. Lee, C. Mattevi, M. Chhowalla, K. Cho and Y. J. Chabal, *Nature Materials*, 2010, **9**, 840.

43 C. Kvarnstrom, H. Neugebauer, S. Blomquist, H. J. Ahonen, J. Kankare and A. Ivaska, *Electrochim. Acta*, 1999, **44**, 2739.

44 C. Kvarnstrom, H. Neugebauer, A. Ivaska and N. S. Sariciftci, *J. Mol. Struct.*, 2000, **521**, 271.

45 A. Dkhissi, F. Louwet, L. Groenendaal, D. Beljonne, R. Lazzaroni and J. L. Bredas, *Chem. Phys. Lett.*, 2002, **359**, 466.

Table of contents entry

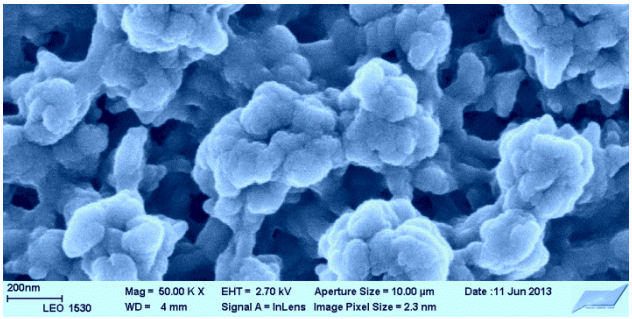

The electrosynthesis of PEDOT in an aqueous dispersion of rGO results in the formation of composite films having a fully open surface morphology.